Mon. Not. R. Astron. Soc. **000**, 000–000 (0000) Printed 17 December 2007 (MN LATEX style file v1.4)

# Jets, plumes and hot spots in the wide-angle tail source 3C 130

M.J. Hardcastle[1⋆,2]

[1] *H.H. Wills Physics Laboratory, University of Bristol, Royal Fort, Tyndall Avenue, Bristol BS8 1TL*
[2] *Mullard Radio Astronomy Observatory, Cavendish Laboratory, Madingley Road, Cambridge, CB3 0HE*



17 December 2007

**ABSTRACT**

I present 1.5- and 8.4-GHz observations with all configurations of the NRAO VLA of the wide-angle tail source 3C 130. The source has a pair of relatively symmetrical, well-collimated inner jets, one of which terminates in a compact hot spot. Archival *ROSAT* PSPC data confirm that 3C 130's environment is a luminous cluster with little sign of sub-structure in the X-ray-emitting plasma. I compare the source to other wide-angle tail objects and discuss the properties of the class as a whole. None of the currently popular models is entirely satisfactory in accounting for the disruption of the jets in 3C 130.

**Key words:** radio continuum: galaxies – galaxies: jets – galaxies: active – galaxies: individual: 3C 130

## 1 INTRODUCTION

3C 130 is a FRI radio source at redshift 0.109 (Spinrad et al. 1985). Its 178-MHz luminosity is $7.6 \times 10^{25}$ W Hz$^{-1}$ sr$^{-1}$, slightly above the nominal FRI-FRII boundary of $\sim 2\times10^{25}$ W Hz$^{-1}$ sr$^{-1}$ (Fanaroff & Riley 1974, hereafter FR). Leahy (1985, 1993) and Jägers and de Grijp (1985) present intermediate-resolution VLA maps of the central regions of the source, while Jägers (1983) has a lower-resolution WSRT image which shows the whole source and its field; the source extends for $\sim 1.5$ Mpc. Saripalli et al. (1996) present high-frequency maps made with the Effelsberg 100-m telescope. The host galaxy is classed as a DE2 by Wyndham (1966) and appears to lie in a cluster, although strong galactic reddening makes optical identification of the cluster members difficult. The *Einstein* detection of extended X-ray emission (Miley et al. 1983), the nearby aligned sources (Jägers 1983) and the many mJy radio sources in the field at 1.5 GHz make it plausible that the object is the dominant member of a large cluster. Leahy (1985) also attempts to constrain the RM distribution of the source, but notes that it depolarizes rapidly (particularly in the S lobe) so that few good measurements are available; this could be taken as evidence for a dense magneto-ionic environment for the source (cf. Hydra A, Taylor et al. 1990).

3C 130 is a wide-angle tail (WAT) radio source. The term WAT has been used to describe many different types of object. Here I shall use it to refer to those FRI sources which are associated with central cluster galaxies (e.g. Owen & Rudnick 1976) and have luminosities comparable to or exceeding the Fanaroff-Riley break between FRI and FRII. I shall follow Leahy (1993) in using the behaviour of the jets at the base as another defining feature. At high resolution one or two well-collimated jets ['strong-flavour' jets, by the classification of Leahy (1993)] are seen (e.g. O'Donoghue, Owen & Eilek 1990), extending for some tens of kpc before broadening, often at a bright flare point, into the characteristic plumes or tails. These jets are very similar to the jets seen in FRII radio galaxies, and quite different from the behaviour of jets in more typical FRIs, where a collimated inner jet, if visible at all, decollimates rapidly (on scales of a few kpc at most) and comparatively smoothly into a bright 'weak-flavour' jet with a large opening angle.[†] WATs, according to this definition, never have a weak-flavour jet, but make the transition between strong-flavour jet and diffuse, bent tail in a single step. The requirement that WATs be central cluster galaxies excludes objects (e.g. 3C 171, Blundell 1996, Hardcastle et al. 1997a; 3C 305, Leahy 1997) where the 'tails' are likely to be simply ordinary FRII lobes which have been disrupted by unusual host-galactic dynamics. The condition on jet behaviour allows us to exclude objects such as the twin sources in 3C 75 (Owen et al. 1985; Hardcastle 1996) which are associated with a dominant cluster galaxy

⋆ E-mail: M.Hardcastle@bristol.ac.uk

[†] There are a few exceptions to this behaviour; 3C 66B (Hardcastle et al. 1996) does appear to show an inner 'strong-flavour' jet and a bright knot at the base of the 'weak-flavour' jet. But even here the transition from strong to weak flavours occurs on scales of $\sim 1$ kpc.

and sometimes classed as WATs but whose inner jets are similar to those of typical powerful FRIs.

Because of the requirements of this definition, wide-angle tail sources make up a small minority of the radio source population. For this reason, the detailed properties of their jets and tails have not been well studied, although a number have been imaged for studies of source dynamics (O'Donoghue et al. 1989). The only objects which have been the subject of detailed study in the radio are 3C 465 (Leahy 1984; Eilek et al. 1984) and 3C 218, Hydra A (Taylor et al. 1990), although M87, Virgo A (e.g. Biretta & Meisenheimer 1993) exhibits some of the properties of a WAT. In this paper I present multi-configuration, multi-frequency VLA observations of a further powerful WAT.

Throughout this paper I use a cosmology in which $H_0 = 50\ \mathrm{km\,s^{-1}\,Mpc^{-1}}$ and $q_0 = 0$. At the distance of 3C 130, one arcsecond is equivalent to a projected length of 2.72 kpc. B1950.0 co-ordinates are used throughout.

## 2 OBSERVATIONS

3C 130 was observed with the VLA as part of a programme of detailed observations of FRI radio galaxies. Dates and integration times are shown in table 1. 3C 286 and 3C 48 were used as primary flux calibrators; the nearby point sources 0537+531 and 0435+487 were used as phase calibrators, and (where 3C 286 was not observed) 3C 138 was used as a polarization angle reference. A bandwidth of 50 MHz was used, except at A configuration, where 25 MHz was used to reduce bandwidth smearing.

The data were reduced within AIPS in the standard way. The datasets from each configuration were initially reduced separately, each undergoing several iterations of CLEANing and phase self-calibration. The B, C and D-configuration datasets were then phase-calibrated, using the appropriate baselines, with images made from the higher-resolution datasets, with which they were then merged without reweighting. Thus the B-configuration data were phase calibrated with an image made from the A-configuration data and merged with it to form an AB dataset; images made with this at low resolution were used to phase calibrate the C-configuration data and the two were merged to form an ABC dataset, and so on. This process ensures phase consistency in the data while removing the need for a self-calibration of the final merged dataset.

Maps were made using the AIPS task IMAGR, with tapering of the *uv* plane where low-resolution maps were required. The robustness parameter in IMAGR was used to temper the uniform weighting of the *uv* plane, to improve the signal-to-noise ratio. In all cases the restoring beam was a circularly symmetrical Gaussian, well matched to the Gaussian fit to the dirty beam, and the resolution quoted is its FWHM. The total-intensity map at the highest resolution was made with a combination of IMAGR and the maximum-entropy imaging task VTESS; IMAGR was used to clean off the bright point-like components, the residual image was deconvolved with VTESS, and the point-like components subsequently restored.

## 3 RESULTS

### 3.1 Overall source structure

Fig. 1 shows the large-scale structure of the source. There are several pronounced bends, in spite of the overall straightness of the source. The sudden change in direction at the end of the south tail is particularly noticeable; this feature is similar to several seen in the small sample of O'Donoghue, Owen and Eilek (1990). The source disappears into the noise on these images and is longer than the $\sim 1$ Mpc seen here.

### 3.2 The core

The radio core of 3C 130 did not vary over the timescales of the observations either at 8.4 or 1.5 GHz, within the errors imposed by the uncertainty of absolute flux calibration at the VLA. Its flux at 8.4 GHz was 29.0 mJy and at 1.5 GHz 12.4 mJy. The best position for the core is RA 04 48 57.34, DEC +51 59 49.7.

### 3.3 The jets and hot spots

The high-resolution images in Figs 2 and 3 show two very well-collimated jets emerging from the core. The jets are reasonably symmetrical. The northern jet in 3C 130 is brighter, noticeably so at bends; over the inner section where both jets are straight (approximately 9 arcsec) the difference in brightness is roughly a factor 1.4. [This symmetry in the brightness of jets is reasonably common among WAT sources, compared to FRII radio galaxies or quasars (e.g. O'Donoghue et al. 1993). The 'archetype' of the class, 3C 465, appears to be unusual in having a very one-sided jet.] The bends in the jets, particularly the northern one, are very striking. The beams may be ballistic, implying some short-timescale wobble of the collimator ('garden-hose' behaviour), but if this is the case it is surprising that the jets are brighter at bends and that there is no antisymmetry between the jet and counterjet. If they are not ballistic it is equally remarkable that they remain collimated while undergoing oscillations of such large amplitude in so short a distance. The northern jet terminates in a hot spot, but there is a long filament which leaves the hot spot to the north, possibly suggesting some continued collimated outflow. At this resolution there is little compact structure at the end of the southern jet; the 'hot spot' seen in the maps of Leahy (1985, 1993) is resolved, with a size of around a second of arc. By contrast, the northern hot spot is only just resolved at the full resolution of the dataset (0.24 arcsec; maps not shown) and its brightest component has a minor axis of $\sim 0.3$ arcsec. This use of the term 'hot spot' is stronger than that of O'Donoghue et al. (1993), who only used it to indicate a brighter, broader region; the hot spot seen here is comparable in compactness with those in nearby FRIIs (e.g. Black et al. 1992; Leahy et al. 1997; Hardcastle et al. 1997a) and is superposed on a brighter region which corresponds to the 'hot spot' of O'Donoghue et al. The northern jet is resolved at the bends at full resolution, and has a cross-sectional width of up to 0.8 arcsec.

The polarization map (Fig. 3) includes a correction for Ricean bias and shows all points with polarized and total intensity greater than three times the respective off-source

r.m.s. noise values. The position-angle vectors are perpendicular to the observed $E$-field, and so show the direction of the apparent magnetic field if Faraday rotation is negligible. Although we expect a non-negligible rotation measure (discussed further below, section 3.4), these angles remain the best guess of the magnetic field direction. On this basis, the jets have apparent magnetic field parallel to their length where polarization is detected; the field follows the bends in the northern jet. This is as expected for a strong-flavour jet (e.g. Saikia & Salter 1988). The field in the hot spot is transverse to the jet direction and parallel to the hot spot's direction of extension; this is similar to the field configuration in many FRII hot spots (Hardcastle et al. 1997a) but also to that in the termination knots of M87's jet (Owen, Hardee & Cornwell 1989). Further out, the magnetic field is parallel to the plumes, and the degree of polarization is high. This appears to be the behaviour in the best-studied WATs (e.g. Taylor et al. 1990, O'Donoghue et al. 1990, Patnaik et al. 1984; Saikia & Salter 1988, and references therein) but is quite different from the behaviour observed in the weak-flavour jets of normal FRIs, in which the field is transverse to the jet axis, sometimes with a longitudinal sheath (e.g. Hardcastle et al. 1996; Laing 1996; Hardcastle et al. 1997b).

### 3.4 Depolarization, rotation measure and spectral index

Using matched-baseline maps, I confirm earlier findings that the source is rapidly depolarized at low frequencies. The mean depolarization between 1.5 and 8.4 GHz (averaged over the areas with good signal-to-noise in both maps) of the northern plume is 0.2, and that of the southern plume 0.1. It may be noteworthy that the southern lobe, with a weaker jet and no bright compact hot spot, is the more depolarized: this may be an example of a Laing-Garrington effect (Laing 1988; Garrington et al. 1988) in WATs, although Saripalli et al. (1996) suggest that there are substantial variations in the degree of polarization with radio frequency. There is weak evidence that the inner 50 arcsec of both lobes is more depolarized than the outer parts, which would be consistent with depolarization by a medium associated with the galaxy or cluster. There are no systematic observations of depolarization in this class of source.

The rotation measure (RM) distribution is not constrained by the rotation of polarization angle between 8.4 and 1.5 GHz. Rotations through all possible angles take place over the source, so there are variations in RM of more than 36 rad m$^{-2}$ on arcsecond scales. This is consistent with the RM measurements of Leahy (1985). Good maps at a higher frequency are needed to constrain the RM distribution adequately. Saripalli et al. (1996) report measurements suggesting an integrated galactic RM of $\sim 300$ rad m$^{-2}$ in the region of 3C 130. From the fact that the polarization vectors are well aligned with one another (and consistent with those in the lower-resolution maps of Saripalli et al.) in the 8.4-GHz maps, and seem to follow bends in the source where these are present, we may guess that the rotation measure towards any point in the source is not much greater than this value, which would produce a 20° rotation in polarization position angle at 8.4 GHz.

The spectral index of the source steepens rapidly with distance from the core. Fig. 4 shows a map of spectral index; the matched baselines of the maps ensure that the steepening is not an effect of undersampling. This spectral behaviour is expected in the standard model in which the plumes flow slowly away from the source [compare the spectral index maps of Hydra A by Taylor et al. (1990)]. Note the comparatively flat ($\alpha \approx 0.5$) spectral index of the jets and of the material they flow into. The northern hot spot has a spectral index flatter than the material that surrounds it.

I determined spectral ages for regions along the (straighter) southern tail, using a minimum energy for the relativistic electron distribution corresponding to $\gamma = 100$, an initial electron-energy power-law index of 2 to reflect the hot spot spectral indices of 0.5, no energy contribution from relativistic protons, filling factor unity, and equipartition magnetic fields; I took flux measurements of regions of the plume between 30 and 110 arcsec, measured along the plume, from the radio core. The ageing field used was 0.46 nT, which was the mean of the equipartition fields fitted at various points along the tail; there was little variation in equipartition field strength with distance, so that this field is a good approximation to the correct self-consistent value. The model included the effects of inverse-Compton scattering from the CBR, which at this redshift produces energy loss equivalent to that due to a magnetic field of 0.40 nT. Using a model with effective pitch-angle scattering of electrons (Jaffe & Perola 1973), the plot of age against projected distance along the source was well fitted by a straight line with gradient $\sim 1.2 \times 10^4$ km s$^{-1}$, inferred ages being of the order of $10^7$ years (as found by Jägers & De Grijp 1985). The intercept was non-zero, reflecting the presence of steeper-spectrum material surrounding the jet termination; derived velocities were similar if the intercept was made zero by choosing a steeper initial power-law index (2.53). These inferred ages and velocities in the tails are comparable to those found by spectral age methods in other WAT sources (e.g. Taylor et al. 1990; O'Donoghue et al. 1993) and would imply outflow which is considerably faster than the sound speed in the external medium, given the temperature of the gas around 3C 130 (discussed below); this is perhaps surprising in view of the absence of any evidence for post-hot spot shock structures in the tails and of their generally relaxed appearance. The usual caveats apply to velocities determined by spectral-ageing methods, but it should be noted that most factors that can affect the velocity (including a contribution to the energy density from relativistic protons, a particle filling factor less than unity, and significant projection of the radio source) will produce velocities higher than the value given above. Only if the assumptions involved in the spectral ageing analysis are seriously wrong – for example, if there is significant *in situ* particle acceleration in the tails or significant magnetic field inhomogeneity – can the tail velocity be much lower than this value. Evidence for such processes is discussed in Eilek (1996) and references therein.

### 3.5 X-ray observations

Miley et al. (1983) report on *Einstein* IPC observations of 3C 130. Serendipitously, the source is also included in the field of a 39.4 ks *ROSAT* PSPC pointed observation, taken from the public archives, of the X-ray emitting supernova

remnant RX 04591+5147 (Pfeffermann, Aschenbach & Predehl 1991; Reich et al. 1992). Although the X-ray source associated with 3C 130 is 32 arcmin away from the pointing centre of the PSPC, and is thus badly vignetted, the observations have superior signal-to-noise to the *Einstein* data and show details of the X-ray structure of the source. The cluster is detected at $2200 \pm 100$ PSPC counts between 0.1–2.4 keV (derived from a circle of 11 arcmin radius about the centre of the X-ray source, using a background annulus between 11 and 17.5 arcmin), in spite of the reduced sensitivity of the PSPC at this off-axis distance. Because of the difficulty of measuring the background in the presence of extended emission from the SNR, and because the shadows of the ring and one of the radial struts pass close to the source, the derived count rate of $\sim 6 \times 10^{-2}$ s$^{-1}$ is uncertain. A rough correction for vignetting would imply an on-axis count rate of $9 \times 10^{-2}$ s$^{-1}$. Using the Post-Reduction Offline Software (PROS) within IRAF, I made spectral fits to the data, correcting for the off-axis location of the source. A single Raymond-Smith model provided a good fit ($\chi^2 = 15.8$ with 26 degrees of freedom), giving a best-fit temperature $kT = 2.9^{+9}_{-2}$ keV; the fitted galactic $N_H$ was $0.9^{+0.5}_{-0.2} \times 10^{22}$ cm$^{-2}$ [cf. the value of $0.4 \times 10^{22}$ cm $^{-2}$ predicted by interpolation from Stark et al. (1992)]. Errors quoted for $N_H$ and $kT$ are $1\sigma$ for two interesting parameters. Abundances were poorly constrained; 70 per cent solar abundance gave marginally the best fit. With this best-fit model, the 0.1-2.4 keV luminosity of the cluster is $5 \times 10^{37}$ W, consistent with the luminosity derived, on crude spectral assumptions, from the *Einstein* data by Miley et al. (1983); the cluster is thus comparable in X-ray luminosity to rich Abell clusters, and the temperature consistent with the temperature-luminosity relation (e.g. David et al. 1993). There is no evidence for a lower temperature in the central regions of the source, and so no evidence that a cooling flow is present; this appears to be normal for the host clusters of WATs (Norman, Burns & Sulkanen 1988; Gómez et al. 1997) although Schindler & Prieto (1997) suggest that a weak cooling flow is present in Abell 2634, the host cluster of 3C 465, and Hydra A inhabits a cooling flow with high mass deposition rates (David et al. 1990).

The best-fit Gaussian to the off-axis point-spread function (PSF) of ROSAT at this distance from the pointing centre has $\sigma \approx 70$ arcsec (Hasinger et al. 1995). For a radio-X-ray comparison I have smoothed the broad-band (0.1-2.4 keV) X-ray image with a Gaussian of this size; this should allow the coma-induced asymmetry of the PSF to be neglected. The X-ray images (Fig. 5) show an extended structure on scales comparable to the length of the radio source (i.e. $\sim 1$ Mpc). The cluster gas seems reasonably symmetrical about the radio source, in contrast to the clumpy structures, with offset radio sources, seen in some lower-luminosity WAT hosts even at lower spatial resolution (e.g. Burns et al. 1994; Gómez et al. 1997). The distortion of the X-ray isophotes to the northeast coincides with, and may be related to, the kink ($\sim$ 150–300 kpc from the nucleus) in the northern tail; there is no structure in the X-ray emission which can be related to the sudden change in direction at the end of the southern radio tail, however. Given the large and asymmetrical PSF, I have not attempted to fit radial profiles to the X-ray data.

## 4 DISCUSSION

Approaches to the source dynamics of WATs in the literature (e.g. Burns 1981; Eilek et al. 1984; O'Donoghue et al. 1993) have concentrated on the large-scale bends seen in the tails. It is instructive to ask a rather different question: why are these sources, with well-collimated strong-flavour jets, compact hot spots, and high radio luminosities, not classical double radio galaxies? In FRII objects of this radio power, radio-emitting plasma is thought to flow back from the hot spots into the 'cocoon' left behind as the hot spot and associated shocks propagate into the external medium, forming the radio lobes (e.g. Scheuer 1974; Williams 1991). In WATs, the jet appears to terminate in a shock in the same way. Norman et al. (1988) argue that strong shocks are necessary to explain the single-step transition between jets and plumes, and observations of compact hot spots in these objects, such as that seen in 3C 130, support this model. However, the situation after the shock is different in the two classes of object. In WATs lobes are not formed. Instead, the hot spot is at the base of the tail; by analogy with the standard model for FRIIs, we may assume that the emitting material in the tail has passed through and been excited in the hot spot, and this is borne out by the spectral index results in 3C 130. The tails may immediately deviate from the axis defined by the jets (e.g. 3C 465) or appear to continue in a straight line (e.g. 3C 130) but in no case does there appear to be lobe emission *significantly* closer to the core than the hot spot.‡ The fact that there is no cocoon may explain the brightness and two-sidedness of the strong-flavour jets in WATs compared to those in FRIIs; a direct interaction with the (comparatively dense) external medium might be expected to make the beam more dissipative and perhaps to slow the regions of the beam responsible for the emission to only weakly relativistic velocities. This would explain the low values ($0.2c$) of 'jet velocity' estimated from sidedness by O'Donoghue et al. (1993) compared to the much higher values ($0.6$–$0.7c$) estimated from the sidedness of jets in FRII quasars (Bridle et al. 1994; Wardle & Aaron 1997) and their prominence and sidedness in FRII radio galaxies (Hardcastle et al. in prep.). Hardcastle et al. (1997a) proposed a similar explanation for the prominence and two-sidedness of the jets in the peculiar FRII 3C 438. However, in the absence of classical double lobes and the associated discontinuity between radio-emitting plasma and shocked external medium, why are there jet termination shocks in WATs?

It is well known that the difference between WATs and classical doubles is the local environment; whereas WATs always lie at the centres of clusters, FRII radio galaxies of comparable powers tend to avoid them (e.g. Prestage & Peacock 1988). An explanation for the peculiar properties of WATs compared to their classical double counterparts must turn on this environmental difference. A suggestion along these

‡ Whether the bends in the jet seen in 3C 130 are due to ballistic motion or to buffeting by the IGM, it is clear that the position of the jet termination point, however it is formed, must change with time. The hot spot will therefore move about in the base of the plume in a manner similar to that described in the 'dentist's drill' model of Scheuer (1982) for the end points in FRIIs. We do not therefore expect to see the hot spot at a particular place in the tail in all cases.

lines by Leahy (1984), applied to 3C 465, invoked motion of the galaxy through the cluster, causing it to leave behind a passive wake of radio-emitting material; in this type of model the post-hot-spot material is left behind by the motion of the galaxy and so never forms a lobe. However, the motions of central cluster galaxies are not expected to be large (Eilek 1984; Pinkney et al. 1993 and references therein) and in any case such a model cannot account, without invoking projection effects implausibly often, for the large population of WATs in which one or both tails are more or less aligned with the inner jets (as in 3C 130).

Burns et al. (1994) suggest a model in which WATs have an origin in the merger of a cluster with a group or subcluster. This is motivated by the X-ray substructure which they find in many WAT host clusters. Large-scale, high-velocity residual motions of gas could then be responsible for the bending of the radio tails, while the merger would provide tidally stripped gas to fuel the AGN. In an extension of this work Gómez et al. (1997) show that the majority of WAT hosts in a larger sample show some X-ray substructure, with an alignment between the direction of the X-ray elongation and the angle that bisects the tails, consistent with such a model. 3C 130, however, is clearly a WAT despite the location of its host at the centre of a smooth, approximately symmetrical distribution of X-ray emitting gas and its (apparently) straight tails. It appears that strong cluster inhomogeneity, though it may be necessary for bent tail formation, is not necessary for the existence of a WAT; in particular it does not, on its own, explain the jet shock/hot spot behaviour discussed above.

Loken et al. (1995) discuss the physics of a jet propagating across the boundary between the interstellar medium of the host galaxy and the hotter, less dense intracluster medium, and suggest that this may be the reason for the disruption of the inner, well-collimated jet at a hot spot. They then postulate velocity shear across the boundary, as described above, to account for jet bending. The structures seen in numerical simulation when the jet simply crosses a contact discontinuity with crosswind do not resemble WATs strongly, however. If the jets are taken to cross a shock front instead (cf. Norman et al. 1988), then the simulations of Loken et al. are more convincing in their resemblance to WATs, but we again face the problem of the smoothness of the large-scale X-ray emission in 3C 130; there is little evidence in this source for the recent cluster merger that Loken et al. invoke to produce such a shock. Neither the sonic radius of a possible cooling flow nor the shock front associated with a putative nuclear or galactic wind are in the appropriate place to produce the internal shocks in WAT jets (Soker & Sarazin 1988; Smith, Kennel & Coroniti 1993). Because of the low resolution of the X-ray data, cluster-merger models cannot be ruled out for 3C 130. Producing such straight plumes in such a model while still causing both jets to disrupt requires a rather special geometry for the merger and/or convenient projection effects, however.

If hot spots in WATs represent jet termination shocks, it is perhaps surprising that only a single hot spot is seen in 3C 130 and that there are no clear hot spot candidates in several of the sources of O'Donoghue et al. (1993). It is possible that there are intrinsically similar hot spots but that relativistic beaming effects are affecting their visibility. In 3C 130 the hot spot in the N lobe is approximately ten times brighter than the most comparable feature in the S lobe, which using standard results requires flow or advance velocities greater than $0.3c$. More high-resolution observations of these objects are needed to test such a model.

## 5 CONCLUSIONS

A compact hot spot is detected at the base of one plume of the WAT 3C 130, and the jets are shown to have longitudinal magnetic field. The source is thus very like a classical double in some respects. The data support the model in which WATs are objects whose jets make the transition from super- to sub-sonic velocities in one step, rather than decelerating gradually, by showing a bright sub-kpc structure (comparable to those seen in classical double radio sources) associated with the termination of a jet.

Archival *ROSAT* PSPC observations of 3C 130 show it to lie in a luminous cluster with $kT \sim 2.9$ keV. There is little sign of substructure in the X-ray, in contrast to many other WATs; this may be related to the nearly straight tails of 3C 130. The lack of strong substructure seems to be inconsistent with recent models for jet disruption in WATs.

## ACKNOWLEDGEMENTS

I am grateful to Julia Riley and Guy Pooley for suggesting the original radio observations of this source, and thank Mark Birkinshaw, Julia Riley and Diana Worrall for useful comments. I acknowledge a research studentship from the UK Particle Physics and Astronomy Research Council (PPARC) and support from PPARC grant GR/K98582. The National Radio Astronomy Observatory is operated by Associated Universities Inc., under co-operative agreement with the National Science Foundation. This project made use of Starlink facilities. This research has made use of the NASA/IPAC Extragalactic Database (NED) which is operated by the Jet Propulsion Laboratory, California Institute of Technology, under contract with the National Aeronautics and Space Administration. This research has made use of data obtained from the High Energy Astrophysics Science Archive Research Center (HEASARC), provided by NASA's Goddard Space Flight Center.

## REFERENCES

Blundell K.M., 1996, MNRAS, 283, 538
Bridle A.H., Hough D.H., Lonsdale C.J., Burns J.O., Laing R.A., 1994, AJ, 108, 766
Burns J.O., 1981, MNRAS, 195, 523
Burns J.O., Rhee G., Owen F.N., Pinkney J., 1994, ApJ, 423, 94
David L.P., Arnaud K.A., Forman W., Jones C., 1990, ApJ, 356, 32
David L.P., Slyz A., Jones C., Forman W., Vrtilek S.D., 1993, ApJ, 412, 479
Eilek J.A., 1996, in Hardee P.E., Bridle A.H., Zensus J.A., eds, Energy Transport in Radio Galaxies and Quasars, ASP Conference Series vol. 100, San Francisco, p. 281
Eilek J.A., Burns J.O., O'Dea C.P., Owen F.N., 1984, ApJ, 278, 37
Fanaroff B.L., Riley J.M., 1974, MNRAS, 167, 31P

Garrington S., Leahy J.P., Conway R.G., Laing R.A., 1988, Nat, 331, 147
Gómez P.L., Pinkney J., Burns J.O., Wang Q., Owen F.N., Voges W., 1997, ApJ, 474, 580
Hasinger G., Boese G., Predehl P., Turner T.J., Yusaf R., George I.M., Rohrbach G., 1995, MPE/OGIP Calibration Memo CAL/ROS/93-015, version 1995 May 08
Hardcastle M.J., 1996, PhD thesis, University of Cambridge
Hardcastle M.J., Alexander P., Pooley G.G., Riley J.M., 1996, MNRAS, 278, 273
Hardcastle M.J., Alexander P., Pooley G.G., Riley J.M., 1997a, MNRAS, 288, 859
Hardcastle M.J., Alexander P., Pooley G.G., Riley J.M., 1997b, MNRAS, 288, L1
Jägers W.J., 1983, A&A, 125, 172
Jägers W.J., De Grijp M.H.K., 1985, A&A, 143, 176
Jaffe W.J., Perola G.C., 1973, A&A, 26, 423
Laing R.A., 1988, Nat, 331, 149
Laing R.A., 1996, in Hardee P.E., Bridle A.H., Zensus J.A., eds, Energy Transport in Radio Galaxies and Quasars, ASP Conference Series vol. 100, San Francisco, p. 241
Leahy J.P., 1984, MNRAS, 208, 323
Leahy J.P., 1985, PhD thesis, University of Cambridge
Leahy J.P., 1993, in Röser H.-J., Meisenheimer K., eds, Jets in Extragalactic Radio Sources, Springer-Verlag, Heidelberg, p. 1
Leahy J.P., 1997, in preparation
Loken C., Roettiger K., Burns J.O., 1995, ApJ, 445, 80
Miley G.K., Norman C., Silk J., Fabbiano G., 1983, A&A, 122, 330
Norman M.L., Burns J.O., Sulkanen M.E., 1988, Nat, 335, 146
O'Donoghue A.A., Owen F.N., Eilek J.A., 1990, ApJS, 72, 75
O'Donoghue A.A., Eilek J., Owen F., 1993, ApJ, 408, 428
Owen F.N., Hardee P.E., Cornwell T.J., 1989, ApJ, 340, 698
Owen F.N., O'Dea C.P., Inoue M., Eilek J.A., 1985, ApJ, 294, L85
Patnaik A.R., Banhatti D.G., Subrahmanya C.R., 1984, MNRAS, 211, 775
Pfeffermann E., Aschenbach B., Predehl P., 1991, A&A, 246, L28
Pinkney J., Rhee G., Burns J.O., Hill J.M., Oegerle W., Batuski D., Hintzen P., 1993, ApJ, 416, 36
Prestage R.M., Peacock J.A., 1988, MNRAS, 230, 131
Reich W., Furst E., Arnal E.M., 1992, A&A, 256, 214
Saikia D.J., Salter C.J., 1988, ARA&A, 26, 93
Saripalli L., Mack K.-.H., Klein U., Strom R., Singal A.K., 1996, A&A, 306, 708
Scheuer P.A.G., 1974, MNRAS, 166, 513
Scheuer P.A.G., 1982, in Heeschen, D.S., Wade C.M., eds, Extragalactic Radio Sources, IAU Symposium 97, Reidel, Dordrecht, p. 163
Schindler S., Prieto M.A., 1997, A&A, 327, 37
Smith S.J., Kennel C.F., Coroniti F.V., 1993, ApJ, 412, 82
Soker N., Sarazin C.L., 1988, ApJ, 327, 66
Spinrad H., Djorgovski S., Marr J., Aguilar L., 1985, PASP, 97, 932
Stark A.A., Gammie C.F., Wilson R.W., Bally J., Linke R.A., Heiles C., Hurwitz M., 1992, ApJS, 79, 77
Taylor G.B., Perley R.A., Inoue M., Kato T., Tabara H., Aizu K., 1990, ApJ, 360, 41
Wardle J.F.C., Aaron S.E., 1996, in Hardee P.E., Bridle A.H., Zensus J.A., eds, Energy Transport in Radio Galaxies and Quasars, ASP Conference Series vol. 100, San Francisco, p. 123
Williams A.G., 1991, in Hughes P.A., ed., Beams and Jets in Astrophysics, Cambridge University Press, Cambridge, p. 342
Wyndham J.D., 1966, ApJ, 144, 459

This paper has been produced using the Royal Astronomical Society/Blackwell Science LaTeX style file.

**Table 1.** VLA observations of 3C 130

| | 8.4 GHz | | 1.5 GHz | |
|---|---|---|---|---|
| Conf. | Date | $t_{int}$ (mins) | Date | $t_{int}$ (mins) |
| A | 1995/08/06[a] | 120 | 1995/07/23[a] | 45 |
| B | 1995/11/28 | 120 | 1995/11/28 | 30 |
| C | 1994/11/10 | 55 | 1994/11/10 | 50 |
| D | 1995/03/06 | 20 | 1995/03/06 | 15 |

[a] Bandwidth of 25 MHz used.
$t_{int}$ denotes the total time spent on source at the specified VLA configuration and frequency.

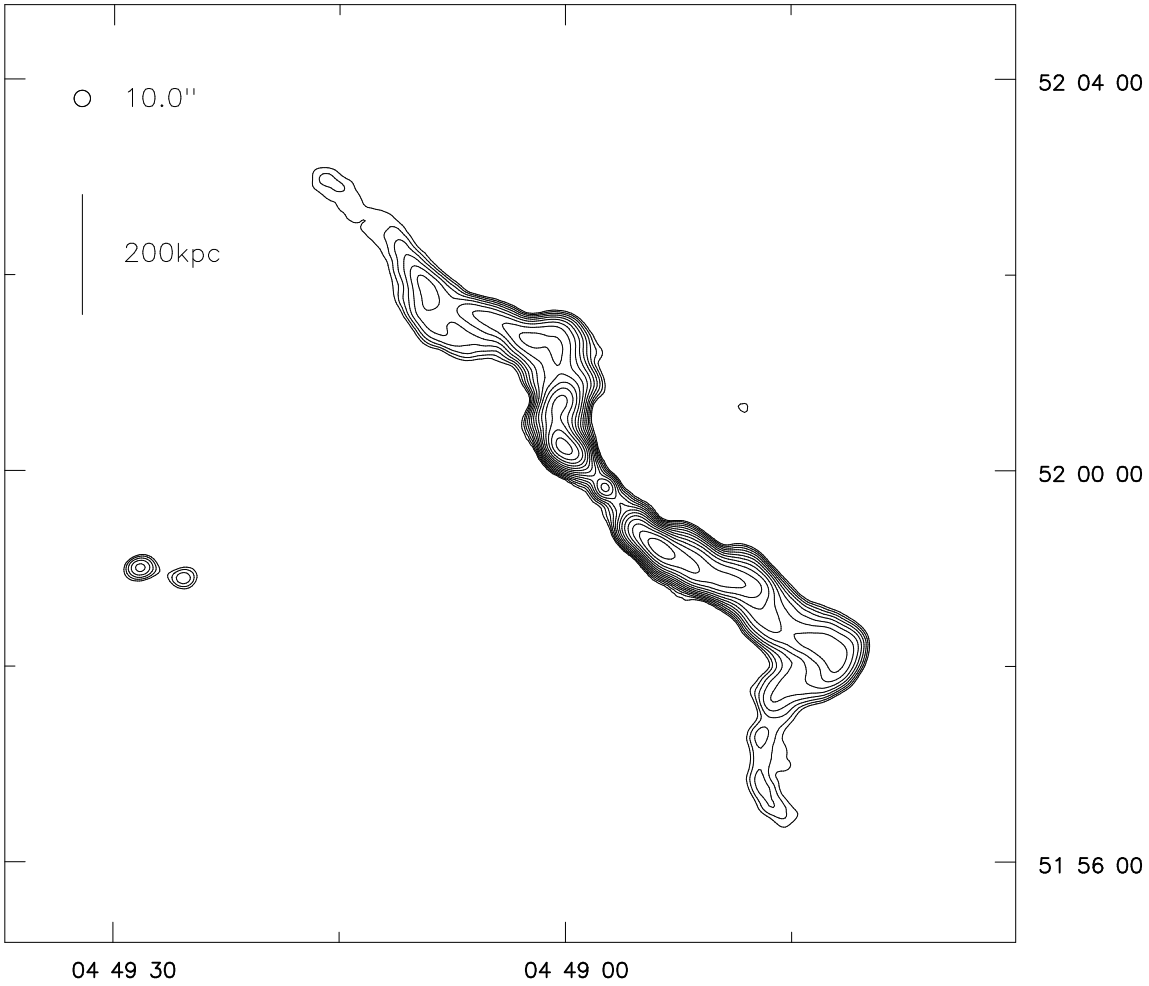


**Figure 1.** 1.5 GHz map of 3C 130 at 10.0-arcsec resolution. Contours at $1.5 \times (1, \sqrt{2}, 2, 2\sqrt{2}, \ldots)$ mJy beam$^{-1}$.

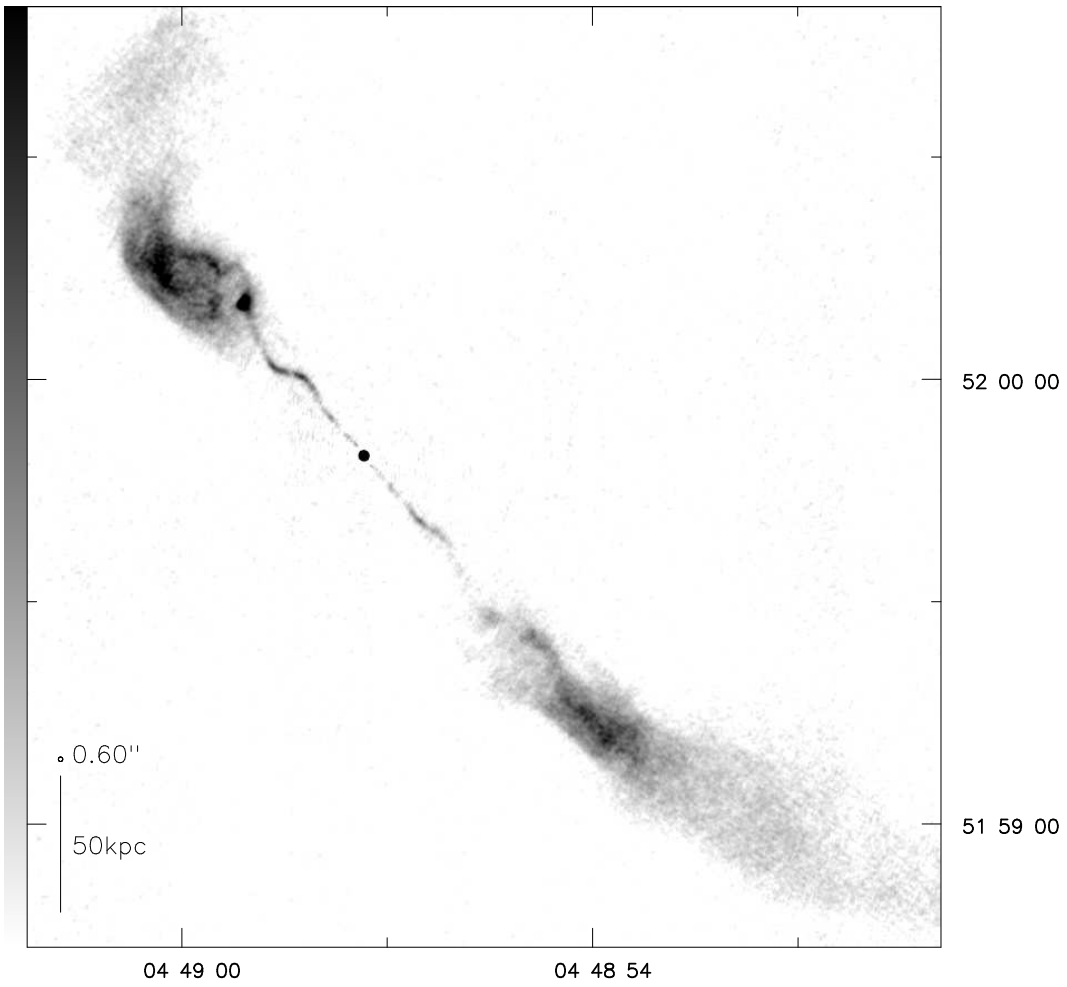


**Figure 2.** 8.4-GHz map of 3C 130 at 0.60-arcsec resolution. Linear greyscale; black is 0.4 mJy beam$^{-1}$.

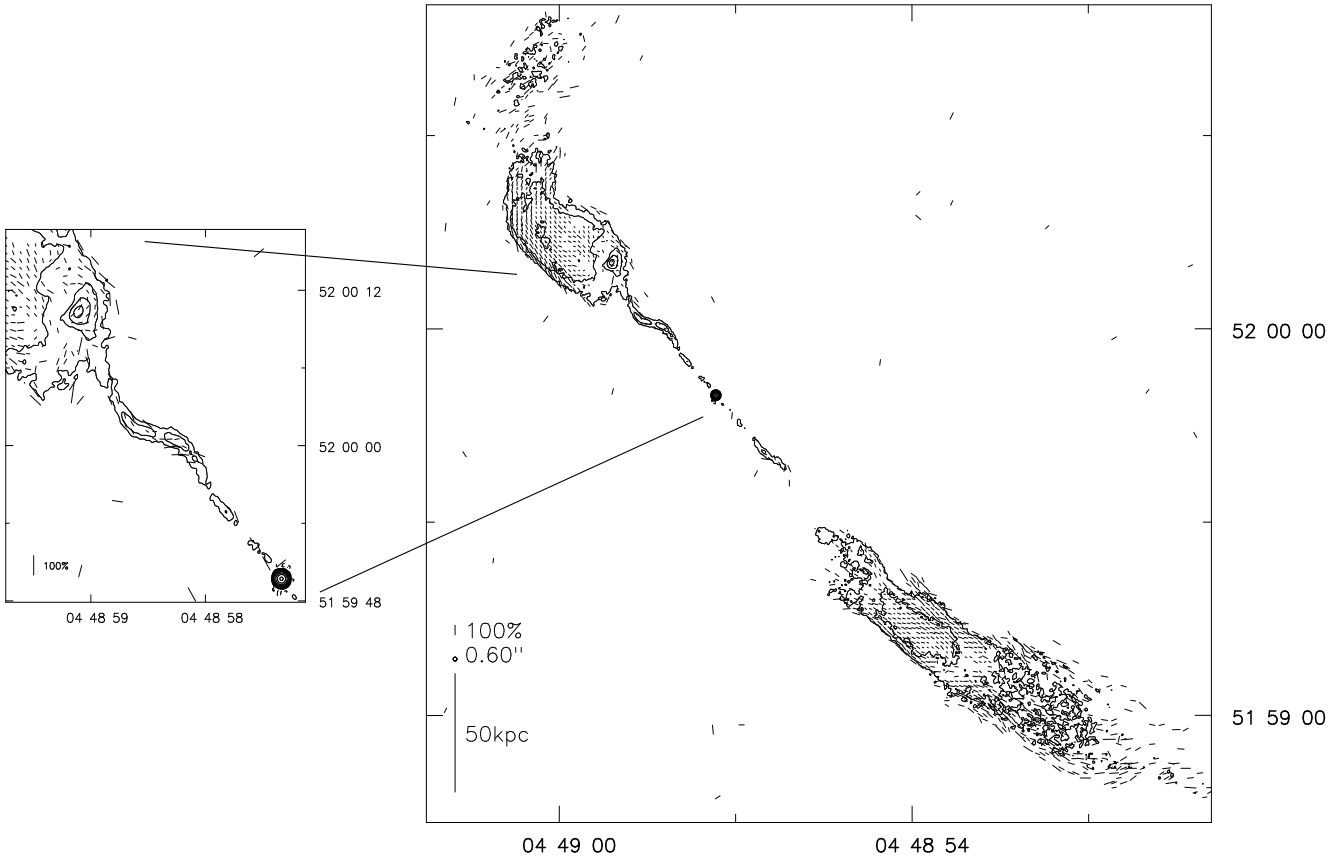


**Figure 3.** 8.4-GHz map of 3C 130 at 0.60-arcsec resolution. Contours at $0.1 \times (-2, -1, 1, 2, 4, \ldots)$ mJy beam$^{-1}$. Vectors show inferred magnetic field direction and their length is proportional to degree of polarization. The inset shows details of polarization in the north jet and hot spot.

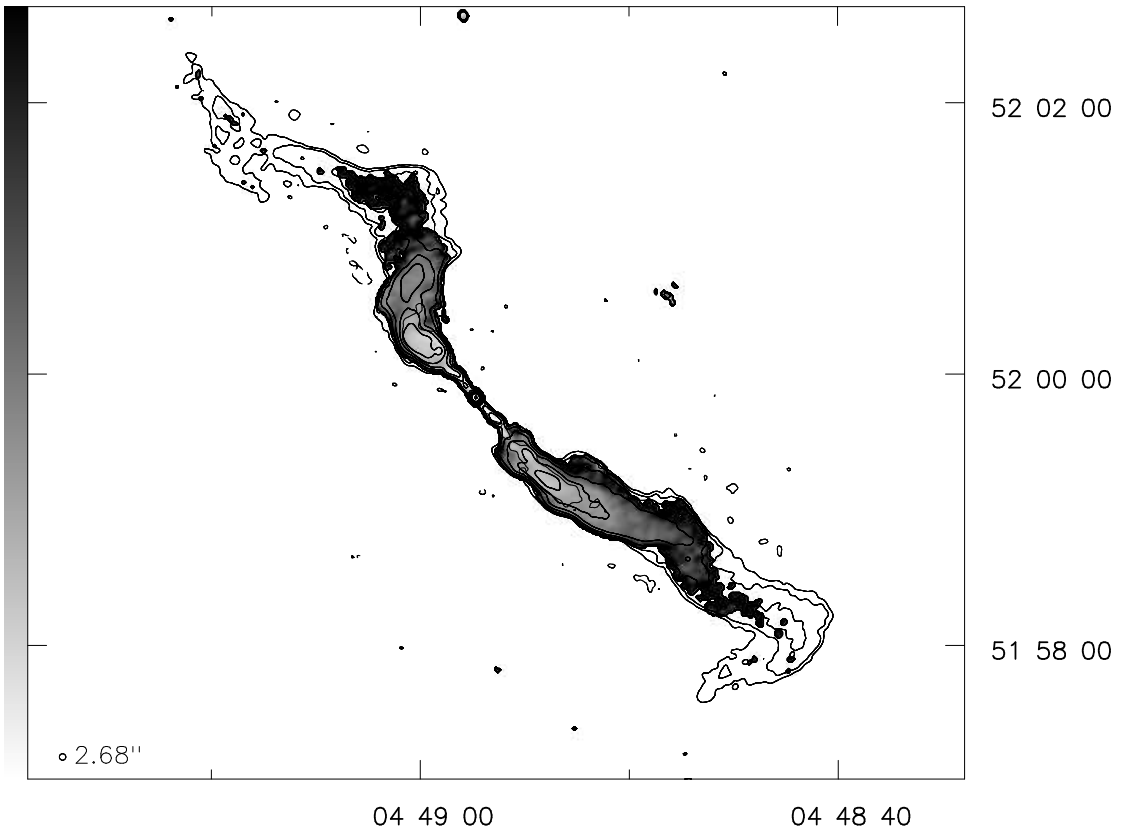


**Figure 4.** Spectral index between 8.4 and 1.5 GHz of 3C 130 at 2.86-arcsec resolution. Linear greyscale between 0.4 and 1.5; superposed are contours of total intensity at 1.5 GHz at $0.4 \times (-2, -1, 1, 2, 4, \ldots)$ mJy beam$^{-1}$.

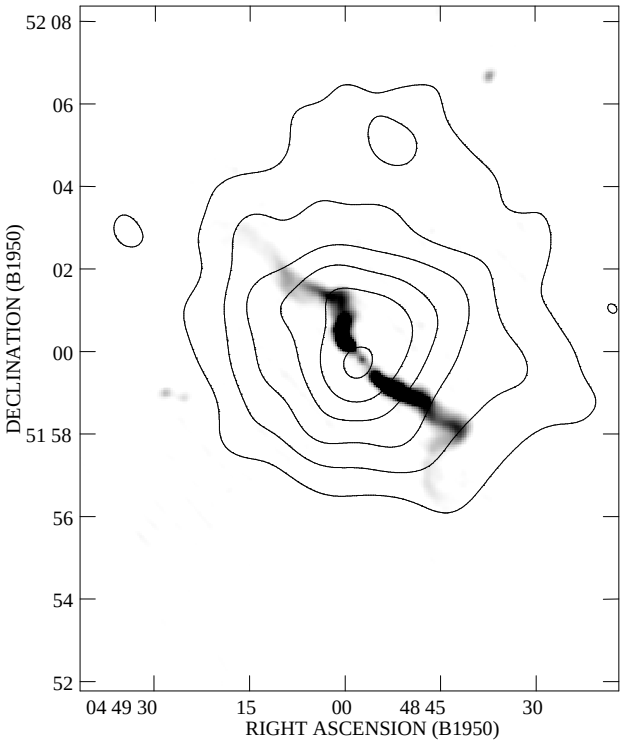


**Figure 5.** X-ray contours of the 3C 130 cluster, smoothed with a $\sigma = 70$-arcsec Gaussian and overlaid on a 10-arcsec resolution greyscale of radio emission at 1.5 GHz (black is 25 mJy beam$^{-1}$). The lowest contour is at background + $3\sigma$ and the contour interval is $2\sigma$. No correction for differential vignetting has been applied; the pointing centre of the PSPC observation was 32 arcmin to the E.